LM-01K081

Hot Isostatic Pressing (HIP) Model Developments for P/M Alloy 690N_2

James W. Sears, Junde Xu

HOT ISOSTATIC PRESSING (HIP) MODEL DEVELOPMENTS FOR P/M ALLOY 690N_2

James W. Sears, Lockheed Martin
and
Junde Xu, Concurrent Technologies Corporation

ABSTRACT

Powder Metallurgy (P/M) Alloy 690N_2, the P/M derivative of Inconel 690 (IN 690), has been shown to have a higher elevated temperature yield strength and superior stress corrosion cracking (SCC) resistance than IN 690. The property improvements seen in P/M Alloy 690N_2 are due to interstitial nitrogen strengthening and precipitation hardening resulting from the formation of fine titanium/chromium - carbo-nitrides. The application of P/M Alloy 690N_2 has had limited use, because of the high costs involved in producing wrought products from powder. Hot Isostatic Pressing (HIP) modeling to produce near net shapes should provide a more economical route for exploiting the benefits of Alloy 690N_2. The efforts involved in developing and verifying the P/M Alloy 690N_2 HIP model are disclosed. Key to the deployment of HIP modeling is the development of the method to fabricate HIP powder containers via laser powder deposition.

INTRODUCTION

Modeling of Hot Isostatic Pressing (HIP) is being developed to optimize the HIP process by predicting the pre-HIP powder container shape to produce near net shape components and thus make the technology more economically attractive for use in industry. Eisen[1] provides a comprehensive review of current research on this topic. A finite element model (FEM) code developed by Concurrent Technologies Corporation (CTC)[2] provides an analytical solution for designing HIP powder container shapes.

This HIP modeling effort is being accomplished through a combination of computer-aided-design (CAD), computer aided manufacturing (CAM), FEM, and laser powder deposition (LPD). The result of the HIP model is a CAD file that represents the optimum powder container design. This file is then translated to a CAM file, which is inputted to a LPD system for powder container fabrication. This process simplifies powder container fabrication for complex internal shapes, eliminates the iterative process in HIP powder container design, eliminates the need for powder container removal (container material is the same alloy as being HIP'd), minimizes secondary machining, and provides a method for improving microstructure through optimized HIP cycle parameters.

Key to the HIP modeling process is the characterization of the powder, semi-consolidated powder (aggregate), and container materials. The powder and semi-consolidated powder were characterized by flow behavior, constitutive functions of the aggregate, thermo-physical properties of the particle, and thermo-physical properties of the aggregate. Flow behavior (simple compression) and thermo-physical properties of the container were characterized. The characteristics of the powder and container materials are inserted into the HIP model.

THE CTC HIP MODEL

The CTC HIP model was originally based on work started by Trasorras, et. al.[3] at Carnegie Mellon University. Trasorras defined two different deformation processes: (1) the deformation of the powder aggregate idealized as a continuum and (2) the deformation of the individual powder particles. The consolidation of powder and accompanying distortion in the powder container can be calculated based on the deformation of the powder compact, which according to viscoplastic law, obeys Equation (1).

$$\dot{\underset{\sim}{\varepsilon}} = \dot{\Lambda}\underset{\sim}{\left(\frac{\partial \Phi}{\partial \sigma}\right)}_{\text{Note 1}} \qquad (1)$$

The Φ can be expressed as follows.

Note 1: $\dot{\underset{\sim}{\varepsilon}}$ is the strain rate tensor, $\dot{\Lambda}$ is the plastic multiplier, $\underset{\sim}{\sigma}$ is the macroscopic stress tensor and Φ is the viscoplastic potential.

$$\Phi = S^2 + b(\rho)p^2 - c(\rho)s^2 \qquad (2)$$

In Equation (2), $b(\rho)$ and $c(\rho)$ are functions of relative density (ρ) and are determined experimentally. The rest of the notations in Equation (2) (S, p, and s) represent loading conditions, S is magnitude of deviatoric stress tensor, p is the negative of the mean macroscopic stress, s is the average magnitude of the deviatoric stress in the powder particle.

$$S=\sqrt{\sigma'_{ij}\sigma'_{ij}}\,,\quad \sigma'_{ij}=\sigma_{ij}+p\delta_{ij}\,,\quad p=-\frac{1}{3}\sigma_{ii}\,,\quad s=\sqrt{\frac{2}{3}}\bar{\sigma}\,,\ \text{Note 2}$$

When the powder aggregate relative density approaches full density, $\rho = 1$, the Φ goes to zero (S = s). Therefore, the functions $b(\rho)$ and $c(\rho)$ must satisfy the limit conditions:

$$\lim_{\rho>1} b(\rho)=0 \quad \text{and} \quad \lim_{\rho>1} c(\rho)=1$$

For dense material, the following viscoplastic (or power law creep) model has been used to quantify the equivalent strain rate $\dot{\bar{\varepsilon}}$ due to temperature θ and stress s.

$$\dot{\bar{\varepsilon}} = A\exp\left(-\frac{Q}{R\theta}\right)\bar{\sigma}^n \qquad (3)$$

In Equation (3), A and n are material constants, Q is the activation energy of the viscoplastic deformation of the material, and R is the universal gas constant.

Shielding Effect

Calibration of the P/M Alloy 690N_2 HIP model involved removing the shielding effect of the carbon steel HIP powder container and quantifying the model to predict powder densification under any complex stress state. Because of the stiffness of the cylindrical container (1015 steel tube), the powder compact within the sealed container only experienced part of the pressure applied to the container's outer surface[4,5]. Therefore, it was necessary to evaluate the shielding effect of the container and find the stress actually transmitted to the powder.

Note 2: $\bar{\sigma}$ is the average flow stress in the powder particle and δ_{ij} is the Kronecker delta)

The applied forces on the cylindrical container in the partial HIP tests include both the applied pressure outside the container and the internal reaction forces of the powder (radial pressure - Σ_R and axial pressure - Σ_Z) being compressed. Since the deformation of the partial HIP containers were measured and the outside pressure prescribed by the HIP cycle, Σ_R and Σ_Z can be calculated through stress analysis of the container.

The calibration was performed through a series of curve fitting exercises to produce the proper analytical form of the two constitutive functions {Equation (2)} and coefficients. These functions (unique for each material) are included in the equation for the Φ that predicts the consolidation of the powder compact.

MECHANICAL AND THERMOPHYSICAL PROPERTIES

Partial HIP and sintered test material was obtained from P/M Alloy 690N_2 powder produced by Crucible Compaction Metals (CCM). This material was tested to determine the mechanical and thermophysical properties under the corresponding HIP parameters (temperature and pressure). Compression tests of cylindrical Alloy 690N_2 powder compact specimens were designed to determine the densification behavior of the material. The thermophysical properties (specific heat and diffusivity) were determined to obtain an accurate relationship between material density, temperature, and thermal conductivity. The data from the partial HIP and sintered P/M Alloy 690N_2 material was used to formulate and calibrate the HIP model by first obtaining the material constants for the viscoplastic model for dense material {Equation (3)}. With the viscoplastic model for dense material calibrated, functions $b(\rho)$ and $c(\rho)$ in Equation (2) can be determined.

Sintering

P/M Alloy 690N_2 powder (-60 mesh) was placed in 1015 carbon steel containers (7" to 12" long, 1.9" outside diameter with 0.204" wall thickness). These containers were open at the top. In each case, a flat disk of 304 SS was placed on top of the powder backed by steel wool. The containers were placed in a vacuum furnace, evacuated ($< 10^{-5}$ Torr), heated to a temperature of 1130°C (2066°F) at a rate of 15°C (27°F)/minute and held for 2 to 4 hours.

The sintered material was sectioned into compression specimens, metallurgical mounts, and cubes for density measurements. The

sintered material densities were not significantly different from the original packing density of the powder. However, sintering the powder produced enough 'green' strength derived from diffusional bonding at powder contact points to produce low density specimens that could be compressed without cracking and thus provide thermophysical data for low density material.

Partial HIP Tests

HIP powder containers (1015 carbon steel, 12" long x 1.9" OD with 0.204" wall thickness) were filled with P/M Alloy 690N_2 powders (same powder as used in sintering). The packing density of the powder in the HIP powder containers ranged from 71.5% to 74.8%. These powder containers were machined with two sets of gage marks 1.00" apart, separated by 6.00". Prior to filling, each powder container was vacuum annealed and helium leak checked. Prior to sealing and outgasing, the powder containers were vibrated to obtain a maximum packing density. Steel wool was inserted to maintain the packing. These powder containers were cold and then hot outgased at 370°C (698°F) to a pressure maintained at $< 1 \times 10^{-6}$ Torr for one hour. The nickel fill tubes on the powder containers were crimped twice, pinched off and seal welded.

These powder containers were HIP'd at 100 MPa (14.5 ksi) and 1130°C (2066°F) according to the HIP schedule shown in Figure 1. The HIP process was interrupted at times of 46, 55, 64, 74, 135, 165, 195, 255, and 315 minutes. Dimensions of the powder containers and distance between the gage marks were measured to determine the total amount of deformation after HIP. Material HIP'd for longer than 74 minutes appeared to be fully dense. Table 1 gives a summary of the density and powder container deformation achieved in these partial HIP specimens.

MECHANICAL AND THERMOPHYSICAL PROPERTY TESTING

Compression tests were performed to determine the viscous nature of the sintered and partially HIP'd material. Thermal diffusivity (α) and specific heat (C_p) were measured to determine thermal conductivity (k) by the equation ($k = C_p \alpha \rho$, where ρ is the density). Cylindrical sintered and partial HIP materials were compression tested at strain rates of 0.1, 0.05 and 0.01 in/min, from room temperature to 1204°C (2200°F). Four specimens were provided from each condition. The combination of sintered material and partial HIP material data gave a broader data space for the equations to function over.

Table 1: List of the P/M 690N_2 partial HIP tests measurements.

HIP Time (minutes)	Outer Radius Shrinkage (%)	Length Shrinkage %	Measured Relative Density	Relative Density Based on Measured Shrinkage on Outer Radius and Length
46	2.37	0.0130	0.715	0.791
55	3.55	0.0273	0.815	0.845
55	3.49	0.0220	0.858	0.856
64	4.71	0.0513	0.91	0.922
≥74	5.76	0.0160	1.00	0.979

Specific heat and thermal diffusivity were determined from four different partial HIP specimens that represented densities of 71.5, 82, 91.5 and 100 percent. The resultant thermal conductivity, as calculated from the specific heat and thermal diffusivity, is plotted as a function of density and temperature in Figure 2.

Viscoplastic Model for Dense Alloy 690

Using the compression test results, the following parameters in Equation (3) were computed with stress in units of ksi and strain rate in 1/second.

$$A = 20775.65 \quad (4)$$

$$Q/R = 32868\ K \quad (5)$$

$$n = 3. \quad (6)$$

Shielding Effect

In the analysis of the container shielding effect in the partial HIP's, the radial and axial shrinkage of the containers were expressed as a continuous function of time based on the experimental measurements. The calculated internal powder reaction pressures (Σ_R and Σ_Z) and the dimensional changes of the containers revealed that there was a considerable shielding effect in both the radial and axial directions as shown in Figure 3. The shielding effect was much larger in the axial direction than in the radial direction because the container was stiffer in the axial direction. Towards the end of powder consolidation, the shielding effect in both directions diminishes. This is reasonable since the powder compact was fully densified and the stress state in the whole specimen approached that of the applied hydrostatic stress state.

Viscoplastic Model for HIP of Porous Alloy 690 Powder

Based on the analysis of the shielding effect and the compilation of dense Alloy 690 properties, from 4, 5, 6 above,

the densification of porous Alloy 690 powder compacts were analyzed to calibrate the constitutive functions $b(\rho)$ and $c(\rho)$ in Equation (2). With ρ_0 ($\rho_0 = 0.715$), it was found that the following expressions provide good agreement with experimental results over the range of temperatures and pressures tested for the densification of Alloy 690.

$$b(\rho) = 2\left(\frac{1-\rho}{1-\rho_0}\right)^3 + 3\frac{(1-\rho)(\rho-\rho_0)}{(1-\rho_0)^2} \quad (7)$$

$$c(\rho) = \rho^{18}\left(\frac{1-\rho}{1-\rho_0}\right) + \rho^{6.5}\left(\frac{\rho-\rho_0}{1-\rho_0}\right) \quad (8)$$

A comparison of the model and experimental results is shown in Figure 4 where the relative density of the Alloy 690 powder compacts from the partial HIP tests is plotted. It can be seen that the calibrated viscoplastic model accurately simulates the densification of the Alloy 690 powder with the exception of the HIP test at 46 minutes. This data was obtained from only one HIP and may be questionable.

HIP MODEL SETUP

The two constitutive functions in the viscoplastic potential that govern the densification of Alloy 690 powder were implemented in a user-code subroutine, UMAT, of the commercial finite element package ABAQUS[6]. The viscoplastic law for dense Alloy 690 was also implemented in the same subroutine. Note that the viscoplastic properties of dense Alloy 690 are simply the properties of the alloy 690 powder with a relative density of unity.

The thermal conductivity and specific heat data of the Alloy 690 powder were inputted as tables in the ABAQUS input data file. Linear interpolation was used to determine the thermophysical properties at any temperature and relative density. The HIP cycle used for the HIP model simulation consisted of simultaneous heating and pressurization in a HIP autoclave to a pressure of 14.5 ksi ±0.5 ksi and a temperature of 1130 °C ± 14°C (2065 °F ± 25 °F) and holding for a period of 240 minutes. This HIP cycle was also implemented in the ABAQUS input data file.

Determination of the HIP Container Shape

A solid model for the demonstration HIP component was set up using the commercial package MSC/PATRAN[7]. Figure 5 shows the design of this component. Using the symmetry of the component

to be manufactured by HIP, only half of the geometry was analyzed. In this case the model consisted of 4063 nodes and 3186 elements. This geometric information was exported to ABAQUS for finite element analysis. The COUPLED TEMPERATURE-DISPLACEMENT analysis option in ABAQUS was used to simulate the coupled heat conduction and powder densification in the HIP consolidation under the applied temperature and pressure. The initial relative density of the Alloy 690 powder compact was 0.715.

To determine the shape for the HIP container that would yield the desired final shape, the following strategy was adopted. Guessing of a container geometry (such as an isotropic expansion of the desired shape), use the finite element analysis to simulate the HIP process and numerically predict the final component shape. Based on the deviation of the predicted geometry from the desired component geometry, modify the input container geometry shape and start a second computer simulation. This estimate-compute-compare-modify (ECCM) loop continues until the deviation between the numerically predicted and desired shape is smaller than a preset tolerance. The flow chart in Figure 6 demonstrates the implementation of the above strategy in determining the computer aided HIP container design.

The fourth simulation produced a HIP container shape solution where no nodes needed modification for a tolerance of ± 0.016". The input container geometry shape from the fourth pass of the ECCM loop was exported from MSC/PATRAN to Pro/Engineer[8]. A native Pro/engineer file (.prt file) was generated for the solid model. From this solid model an .stl file was created for further use in LPD fabrication.

HIP DEMONSTRATION

The .stl file generated from the computer aided HIP container design was used as input for the LPD fabrication. The LPD process slices the .stl file into thin (0.010" to 0.030") layers and exports them to a CAD interface that drives the laser powder deposition head[9]. Figure 6 shows the process of HIP powder container fabrication starting with the container design by modeling, prototype fabrication using fused deposition modeling (FDM), LPD HIP container fabrication, HIP processing the powder filled container, and the final machining of the HIP'd component. This HIP fabrication represents the first structure fabricated directly from a model-based approach incorporating the LPD powder container fabrication technique.

Figure 8 shows the comparison between the HIP'd structure produced by the modeling process and the original designed shape. To obtain these measurements the HIP'd demonstration component was cut into one inch long segments. Measurements were taken from the interface of each of these segments. No internal dimension deviated more than 0.050" and most errors were less than 10 percent.

The source of errors in this process may be attributed to the tolerances used in the HIP model simulations, original packing density of the powder, the ability of the model to exactly predict the powder consolidation and the ability of the LPD process to accurately produce the powder container shape.

CONCLUSIONS

It is recognized that the tolerance used in determining the container shape is somewhat tentative. Indeed, proper choice of the tolerance in computer aided design depends on how accurately the LPD can be controlled and the tolerance given by the component design. This issue remains open for the time, but it will be resolved when experience is accumulated through industrial HIP practice.

Laser powder deposition is capable of producing HIP powder containers having complex shapes thus making it possible to fabricate net shape components through HIP. The technique adopted for this work, together with the HIP modeling system, provides an efficient approach to determine the correct HIP powder container shape. This technique can also be applied as an additive manufacturing step for producing hybrid structures made from simple inexpensive wrought shapes and more complex value added HIP'd powder shapes. This is possible since through HIP modeling the composite, a HIP container can be designed and the LPD process can be used to fabricate the powder container onto the simple wrought shapes.

REFERENCES

1. W.B. Eisen, "Mathematical Modeling of Hot Isostatic Pressing", Reviews in Particulate Materials, Volume 4, 1996, pp. 1-42.

2. R.E. Smelser, J.F. Zarzour, J. Xu, and J.R.L. Trasorras, "Modeling of Near Net Shape Hot Isostatic Pressing", Mechanics in Materials Processing, ASME, 1994.

3. J.R.L. Trasorras, M.E. Canga, and W. Eisen, "Modeling the Hot Isostatic Pressing of Titanium Parts to Near-Net-Shape", Advances in Powder Metallurgy & Particulate Materials - 1994, Vol. 7, pp. 51-69.

4. J. Xu and R.M. McMeeking, "An analysis of the Can Effect in an Isostatic Pressing of Copper Powder", Int. J. Mech. Sci., Vol. 34, No. 2, pp. 167-174, 1992.

5. H.N.G. Wadley, R.J. Schaefer, A.H. Kahn, M.F. Ashby, R.B. Clough, Y. Geffen and J.J. Wlassich, "Sensing and Modeling of Hot Isostatic Pressing of Copper Powder", Acta Metall. Mater., Vol. p. 979, 1991.

6. ABAQUS is a registered trademark of Hibbitt, Karlsson and Sorenson, Inc.

7. MSC/PATRAN is a registered trademark of the MacNeal-Schwendler Corporation.

8. Pro/Engineer is a registered trademark of Parametric Technology Corporation.

9. J.W. Sears, "Direct Laser Powder Deposition - State of the Art", *Powder Materials: Current Research and Industrial Practices*, Proceedings of the 1999 Fall TMS Meeting, ed. by F.D.S. Marquis, November 1999, pp. 213-226.

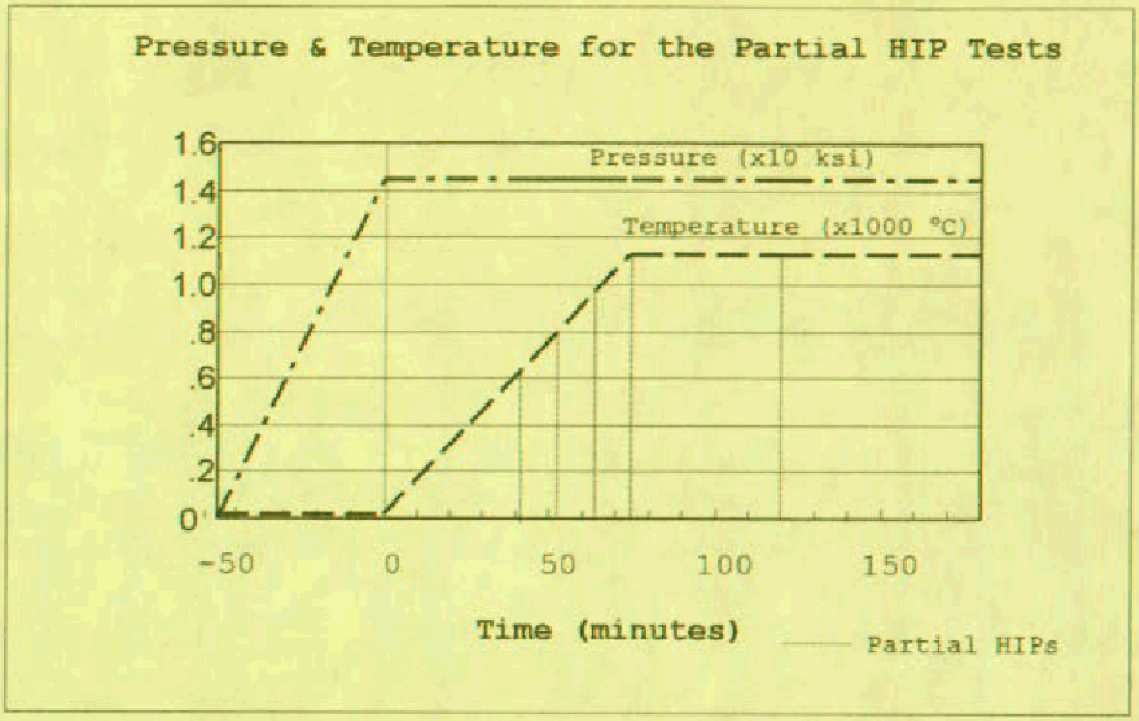

Figure 1: Schematic of the HIP cycle used for the partial HIP tests.

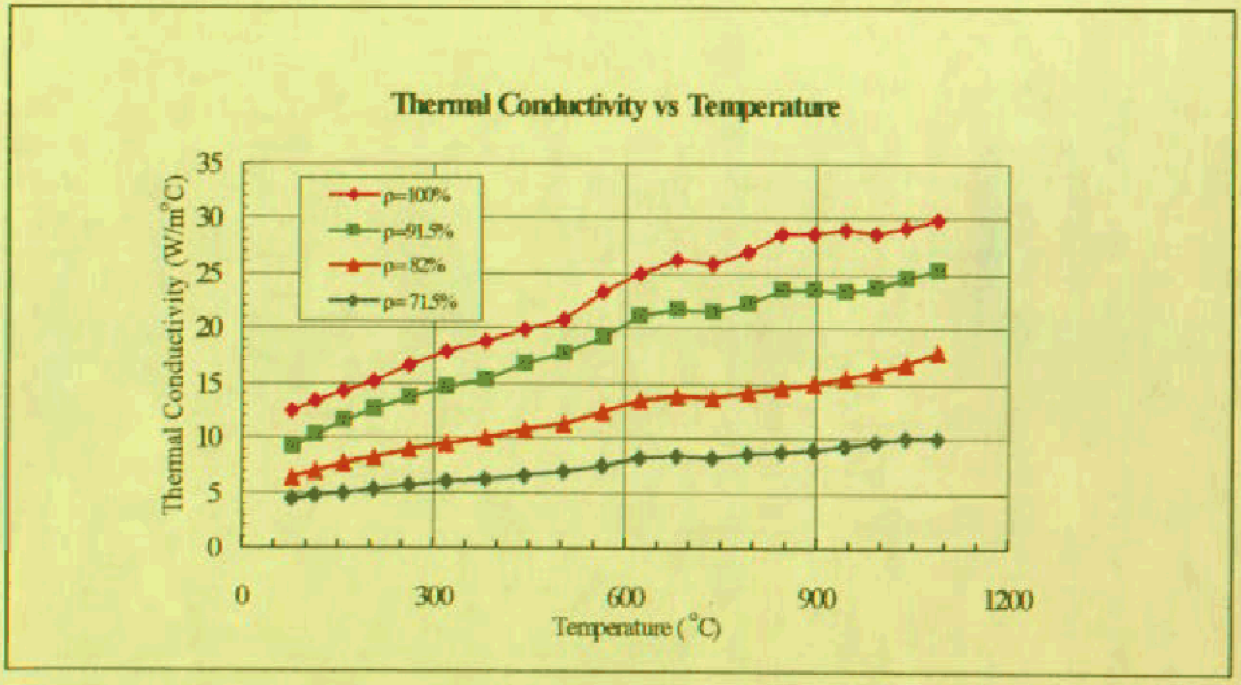

Figure 2: Thermal Conductivity plotted as a function of temperature for various densities of P/M Alloy 690N_2.

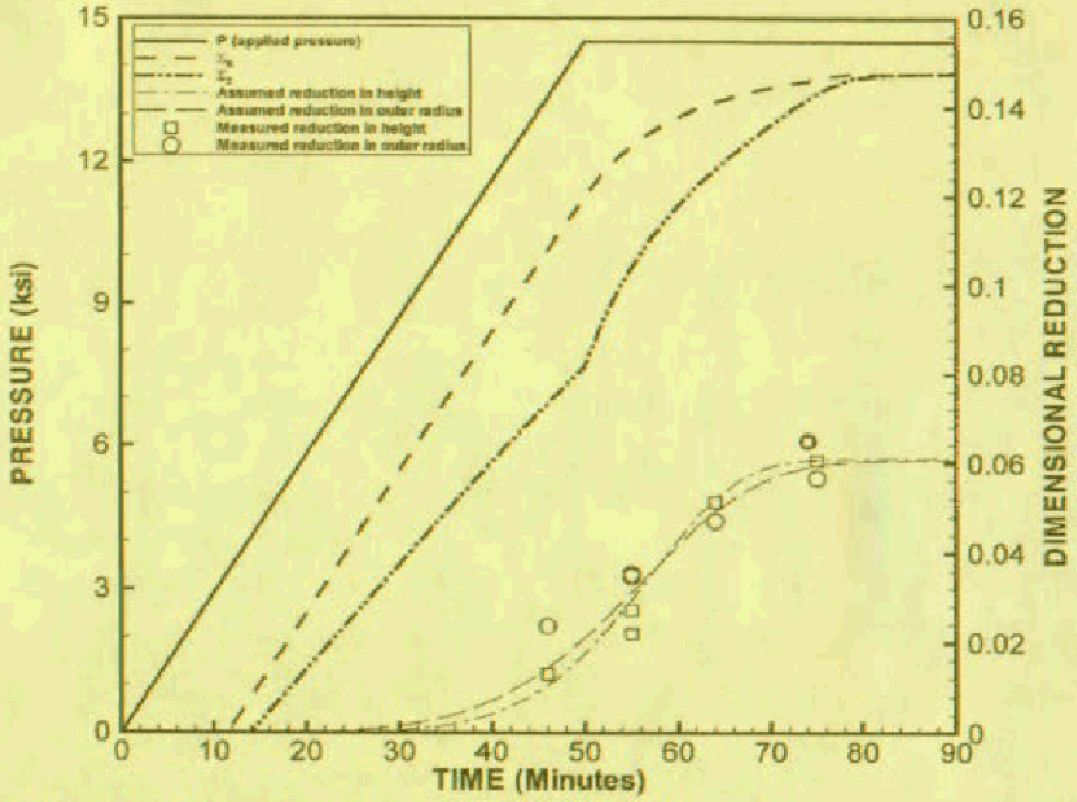

Figure 3: Results from Container Shielding Effect Analysis

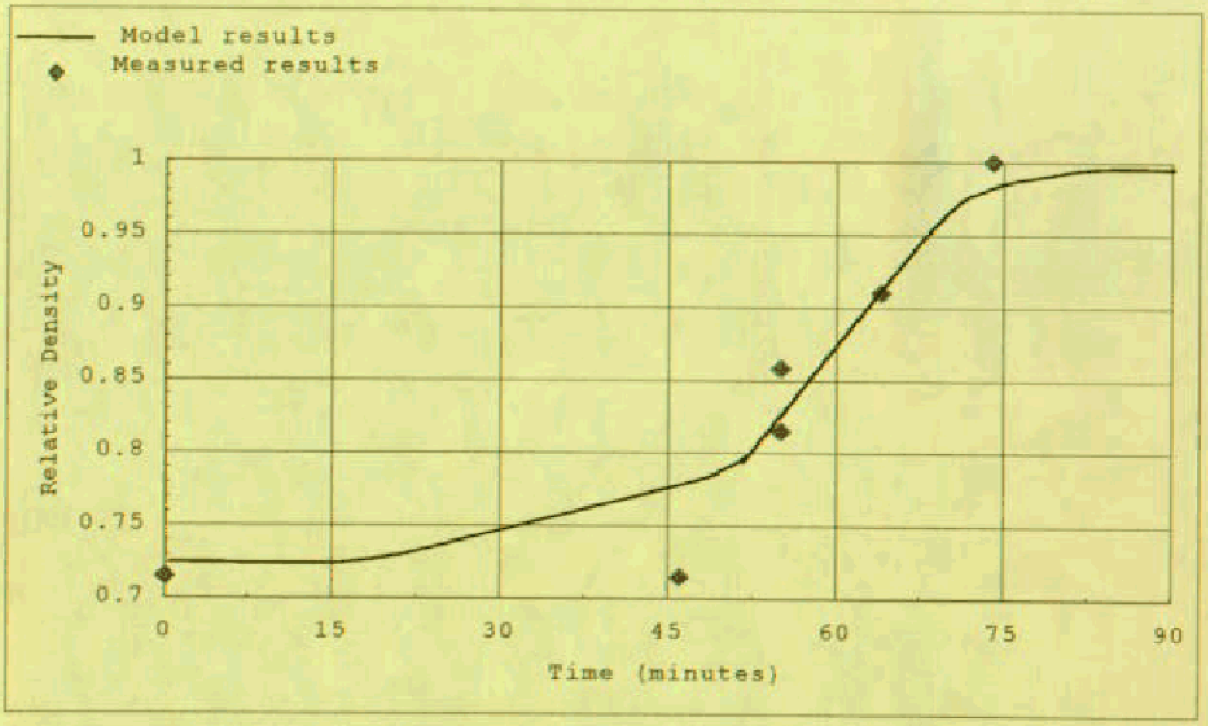

Figure 4: Comparison of results from model relative density and partial HIP tests data.

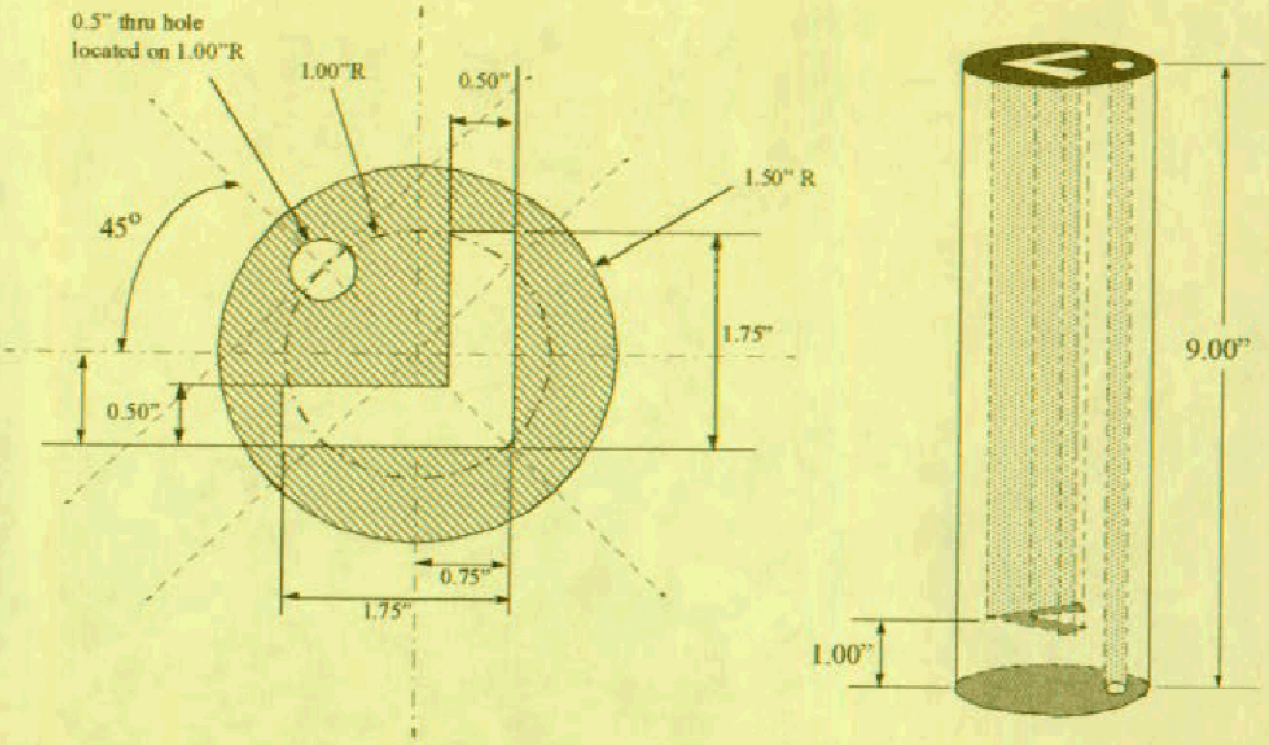

Figure 5. Design of the demonstration HIP component.

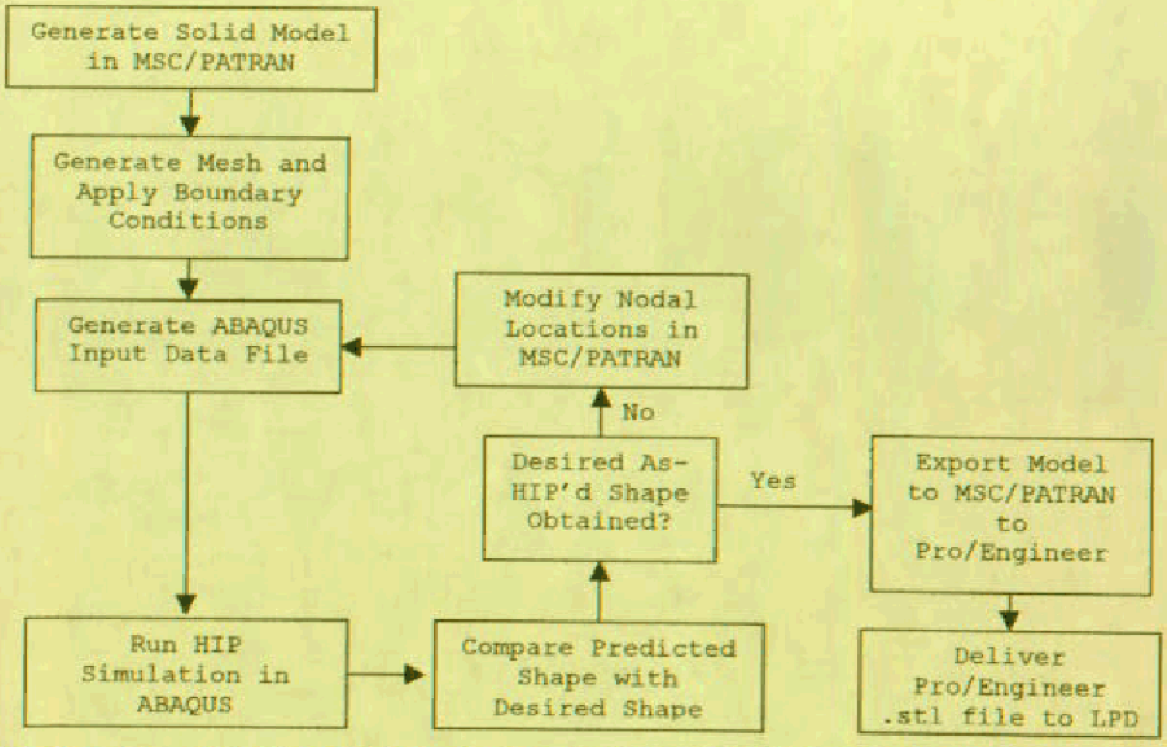

Figure 6: Strategy for determining initial container

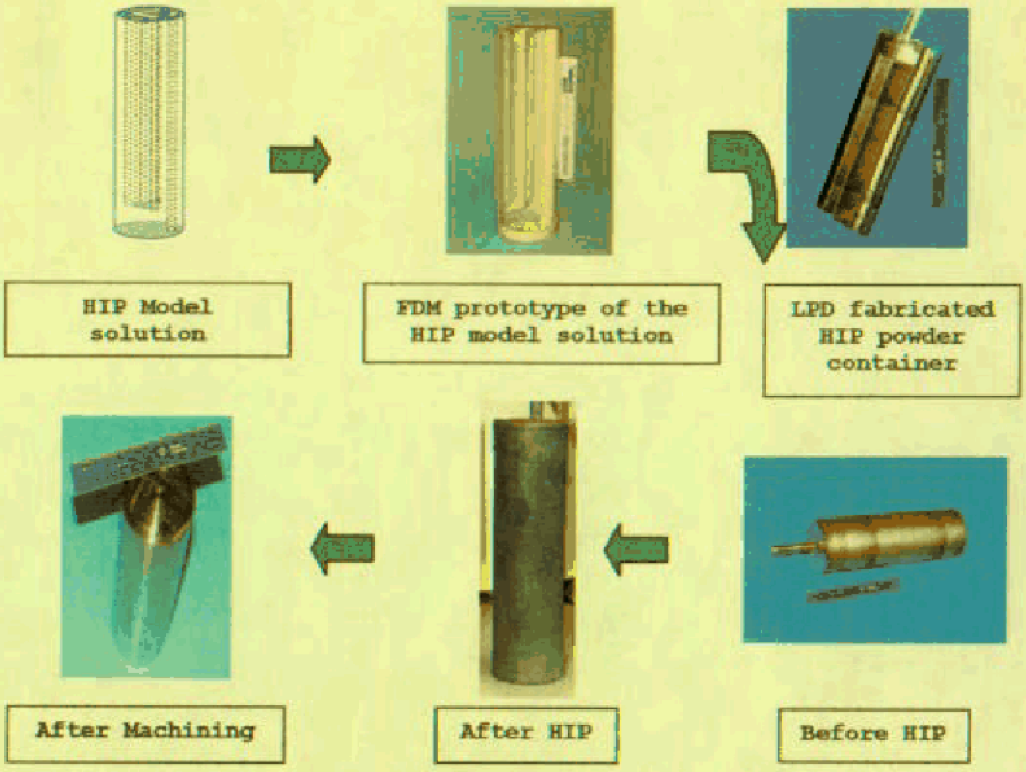

Figure 7: The FDM prototype, the LPD fabricated HIP powder container, the as-HIP'd demo shape and the HIP'd demo after machining produced during the first HIP demonstration.

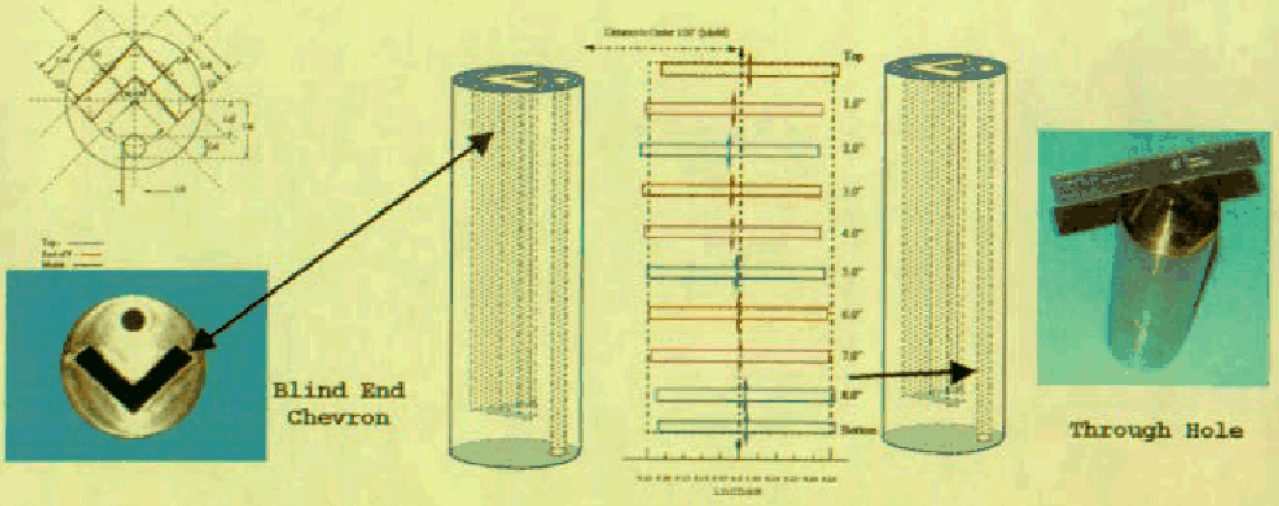

Figure 8: A comparison between the model produced HIP'd shape and the original design, the blind-end chevron and the through hole.